Photoinduced Energy Transfer in Carbazole-BODIPY Dyads

Journal:	*Physical Chemistry Chemical Physics*
Manuscript ID	CP-ART-08-2018-005509.R1
Article Type:	Paper
Date Submitted by the Author:	29-Sep-2018

Complete List of Authors:	Lingamallu, Giribabu; Indian Institute of Chemical Technology, Polymers & Functional Materials Division Reddy, Govind; CSIR-Indian Institute of Chemical Technology, Polymers & Functional Materials Division Duvva, Naresh; CSIR-Indian Institute of Chemical Technology, Polymers & Functional Materials Division Seetharaman, Sairaman; University of North Texas DSouza, Francis; University of North Texas, Department of Chemistry

Journal Name

ARTICLE

Photoinduced Energy Transfer in Carbazole-BODIPY Dyads

Received 00th January 20xx,
Accepted 00th January 20xx

DOI: 10.1039/x0xx00000x

www.rsc.org/

Govind Reddy,[a] Naresh Duvva,[a] Sairaman Seetharaman,[b] Francis D'Souza[b*] Lingamallu Giribabu[a*]

A series of carbazole (CBZ)-boron dipyrromethene (BODIPY) based donor-acceptor dyads, **CB1**, **CB2**, and **CB3**, in whichCBZ as an energy donor, tethered together with spacers of varied sizes *i.e.*, phenyl bridge, biphenyl bridge and diphenylethyne bridge, respectively, are reported. The newly synthesized dyads were characterized by various spectroscopic techniques.A comparison of the absorption and electrochemical data of the dyadswith their reference compounds (*i.e.*, 9-Phenyl-9H-carbazole(**C0)** and *N,N´*-difluoroboryl-1,3,7,9-tetramethyl-5-phenyldipyrrin**(B0)**) revealed minimal ground-state interactions betweenchromophores. Selective excitation of CBZ in the dyads at 290 nm resulted in quenching of the CBZ emission followed by the appearance ofBODIPY emission revealing efficient energy transfer from singlet excited CBZ (^{1}CBZ*) to BODIPY.The photoinduced energy transfer phenomenon was studied in three different solvents of varying polarity. The driving forces of energy transfer (ΔG_{EN}) for all the dyads were found to be exothermic. The rate constants for energy transfer, k_{ENT}, measured from femtosecond transient absorption technique in toluene were found to be in the range of 0.8-2.0x 10^{10} s^{-1}, depending on the type of spacer between the CBZ and BODIPY entities, and were in close agreement with the theoretically estimated rates according to Försterenergy transfer model. In contrast, selective excitation on BODIPY in these dyads at 485 nm resulted small quenching of BODIPY emission suggesting lack of major photochemical events originating from ^{1}BODIPY*.

Introduction

Artificial photosynthesis (AP) is a process of mimicking natural photosynthesis for effective conversion of light energy into a more accessible forms of energy.[1-6] By studying the natural phenomenon as it occurs in plants and bacteria, the scientific community started designing different multichromophoric arrays for use in energy conversion.[7-12] These APs consist of three main components; a photo antenna, a reaction centre and an energy storage system. The antenna unit plays a key role in the absorption of light, the excitation and transfer of electrons from donor to acceptor for long-lived charge separation. Charge separation has the necessary criteria in the natural photosystem, whereas light energy absorbed by various types of chlorophyll molecules initiated the electron transfer and subsequent charge separation to make the first move for photosynthesis.[13]During past decades, several molecular and supramolecular donor-acceptor systems have reported in the literature that mimic the primary events of natural photosynthetic machinery by displaying photoinduced energy transfer (PEnT) and photoinduced electron transfer (PET) processes, converting the solar energy to electricity.[14-19] Despite considerable progress has been made in this area, designing new systems that differ from preceding ones in photoactive unit, linker, spatial arrangement etc., has a great demand because of their applications also inconstructing optoelectronic devices.[20-23]

Owing to their close resemblance to natural pigments, chlorophylls and bacteriochlorophylls, and relatively easy synthetic manipulations, porphyrin as the primary photoactive entity has dominated this area of research.[24,25]In addition, porphyrin-like molecules with rich photo- and redox properties, viz., phthalocyanines,[26,27] corroles,[28,29] N-confused porphyrins,[30] expanded porphyrins[31] and BODIPYs[32] etc., have also been successfully utilized in the construction of D-A systems.Of these, BF_2-chelated dipyrromethenes*i.e.*, 4,4-difluoro- 1,3,5,7-tetramethyl-4-bora-3a,4a-diaza-s-indacene (abbreviated as BODIPYs)are versatile functional dyes with high stability and favourable photophysical and electrochemical properties, which can be tuned readily through chemical modification of the BODIPY core.[33]Generally, BODIPYs exhibit large molar extinction coefficients ($\varepsilon \approx 10^5$ M^{-1} cm^{-1}) with absorption maxima around 500 nm, comparatively high fluorescence quantum yields (0.57 in CH_2Cl_2), and

[a.] *Polymers & Functional Materials Division, CSIR-Indian Institute of Chemical Technology, Habsiguda, Hyderabad-500007, (Telangana), India .Email: giribabu@iict.res.in. Phone: +91-40-27191724, Fax: +91-40-27160921*

[b.] *.Department of Chemistry, University of North Texas, 1155 Union Circle, #305070, Denton, TX 76203-5017, USA Email: francis.dsouza@unt.edu*

[c.]

† Electronic Supplementary Information (ESI) available: ^{1}H NMR and ESI-MS spectra,cyclic voltammograms, fluorescence spectra, optimized structure, frontier molecular orbitals, and transient absorption spectra] See DOI: 10.1039/x0xx00000x

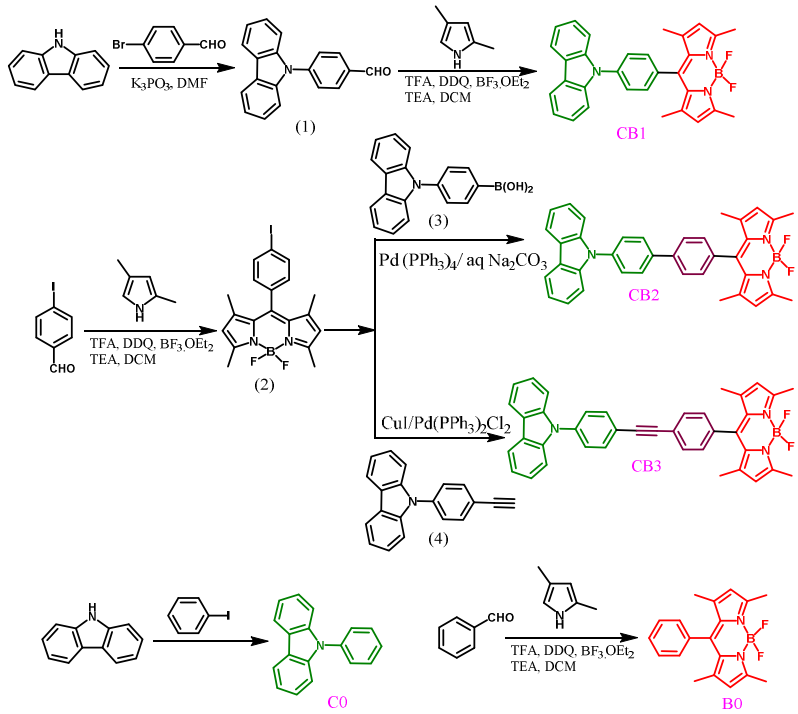

Scheme 1: Synthesis of **CB1**, **CB2**&**CB3** and controlled compounds **C0**&**B0**

relatively long-lived singlet excited states (4-6 ns).[34]As a result, they have been extensively used as energy-absorbing and transferring antenna molecules in photosynthetic antenna-reaction centre mimics.[35,36] On the other hand, organic molecules having complementary absorption to BODIPY have particularly interested for the construction of D-A systems. In this regard, carbazole molecule having absorption in the UV region is found to be an appealing candidate for the construction of D-A systems. Carbazole is a heterocyclic organic compound having absorption in the 300-400 nm region and has been extensively utilized in optoelectronic applications.[37,38]

In the present study, we have designed donor-spacer-acceptor systems involving carbazole covalently connected to BODIPY.We have explored detailed synthesis, spectroscopic characterization and photophysical properties of Carbazole-BODIPY based dyadsin which photo-induced events with respect to the spacer type and sizes are reported. These studies are very essential not only to understand the photophysical events of natural photosynthesis but also the concepts used for the design of efficient materials for optoelectronic applications. In the present study, the synthesized CBZ-BODIPY dyads, **CB1**, **CB2**, and **CB3** are tethered together with varied spacer types and sizes *i.e.*, phenyl bridge, biphenyl bridge and diphenylethyne bridge, respectively. The molecular structures and syntheses of the dyads (**CB1**, **CB2**, and **CB3**) and the control compounds (**C0** and **B0**) are shown in Scheme 1.

Experimental

from Sigma-Aldrich orMerck. Analytical reagent (AR) grade solvents were used for the reactions while laboratory reagent (LR) grade solvents were used for sample purifications and column chromatography. Dichloromethane, chloroform, and acetonitrile were driedin the presence of calcium hydride under a nitrogen atmosphere. Toluene and tetrahydrofuranwere purified by refluxing the solvents overnight in the presence of Na metal added benzophenone, followed by distillation under vacuum. The purified solvents were stored over 4Å molecular sieves. Triethylamine was distilled over NaOH pellets. ACME silica gel (60-120 mesh) was used for column chromatography. Thin layer chromatography was performed on Merck-precoated silica gel 60-F254 plates. Either gravity or flash chromatography was performed for purification of all compounds. All the reactions were carried out under nitrogen or argon atmosphere using dry and degassed solvents.

Synthesis

4-(9*H*-Carbzol-9-yl)benzaldehyde**(1)**,[39] 9-Phenyl-9H-carbazole **(C0)**,[40] *N,N´*-difluoroboryl-1,3,7,9-tetramethyl-5-phenyldipyrrin (**B0**),[41] 4-(9H-**,**4,4-Difluoro-8-(4'-iodophenyl)-1,3,5,7-tetramethyl-4-bora-3a,4a-diaza-s-indacene (Iodo-BODIPY)**(2)**,[42] were synthesized according to the literature procedures.

Synthesis of CB1. 2,4-dimethylpyrrole (0.154 g, 1.623mmol) and **1** (200 g, 0.738 mmol) were dissolved in dry CH_2Cl_2 (200 ml) under N_2 atmosphere. One drop of TFA was added and the solution was stirred at room temperature for 2 h. At this point, a solution of DDQ (0.251 g, 1.107 mmol) in 50 mL dry

$CH_2Cl_2$was added, stirred for 1h followed by the addition of Et_3N (1.023 mL, 7.38 mmol) and $BF_3.OEt_2$ (0.73 mL, 5.904 mmol). After 30 min., the reaction mixture was extracted in CH_2Cl_2 and the organic layer was dried over anhydrous Na_2SO_4. Evaporation of the solvent under reduced pressure gave the crude product, which upon purification by silica gel column chromatography using dichloromethane/hexane (1:1 v/v) as eluent gave the titled compound as a red solid. Yield: 18%. ^{1}H NMR (400 MHz, $CDCl_3$) δ 8.17 (d, J = 7.7 Hz, 2H), 7.75 (d, J = 7.4 Hz, 2H), 7.58 (d, J = 7.1 Hz 2H), 7.45 (ddd, J = 8.2, 7.0, 1.2 Hz, 2H), 7.39 (d, J = 8.1 Hz, 2H), 7.33(m, 2H), 6.06 (s, 2H), 2.59 (s, 6H), 1.60 (s, 6H).^{13}C NMR (100 MHz, $CDCl_3$) δ 155.79, 142.70, 140.60, 138.44, 134.12, 131.45, 129.83, 127.83, 126.17, 123.62, 121.57, 120.53, 120.37, 109.44, 46.72, 29.72, 14.67, 8.68. MALDI-MSCalcd.m/z ($C_{31}H_{26}BF_2N_3$) 489.37, Found 489.17 (40%).

Synthesis of CB2. Under N_2 atmosphere, a mixture of compound **3**(0.100g, 0.348mmol), compound **2** (0.150 g, 0.348mmol), Pd(dppf)Cl_2 (17.06mg, 0.02mmol), 2 M aqueous solution of Na_2CO_3 (2 ml) in dry THF (15 ml) was refluxed overnight. The reaction mixture was extracted inDCM, and washed with water and brine solutions. The organic layer was dried with anhydrous Na_2SO_4 and then the solvent was removed by rotary evaporation. The residue was purified by column chromatography on silica gelusing Hexane and DCM in the ratio of 6:4 (v/v) as the eluent to give corresponding compound **CB2** (Yield: 65%). ^{1}H NMR (400 MHz, $CDCl_3$) δ 8.17 (d, J = 7.7 Hz, 2H), 7.93 (d, J = 8.4 Hz, 2H), 7.86 (d, J = 8.1 Hz, 2H), 7.70 (d, J = 8.4 Hz, 2H), 7.51 – 7.40 (m, 6H), 7.31 (t, J = 7.2 Hz, 2H), 6.02 (s, 2H), 2.58 (s, 6H), 1.49 (s, 6H). ^{13}C NMR (100 MHz, $CDCl_3$) δ 157.15, 146.70, 140.79, 139.30, 134.40, 128.77, 128.47, 127.62, 127.52, 126.03, 123.52, 121.34, 120.41, 120.12, 109.56, 41.49, 29.71, 14.14, 8.06. MALDI-MS Calcd.m/z ($C_{37}H_{30}BF_2N_3$) 565.46, Found 565.18 (100%).

Synthesis of CB3. Under N_2 atmosphere, to a mixture of compound **2**(50 mg, 0.124 mmol), compound **4** (66mg, 0.248mmol), $AsPPh_3$ (76mg, 0.248mmol), $Pd_2(dba)_3$ (34mg, 0.037mmol), triethylamine (1 mL), 10 mL of THF was added from an addition funnel. The reaction mixture was warmed to 30^{0}C with stirring for 30 min and at room temperature for 20 - h. Analysis of the reaction mixture by TLC indicated the completion of the reaction. After removal of the solvent, the residue was purified on silica gel column (hexane–DCM: 6/4) as eluent to give corresponding compound **CB3** (Yield: 48%). ^{1}H NMR (400 MHz, $CDCl_3$) δ 8.15 (d, J = 7.7 Hz, 2H), 7.79 (d, J = 8.5 Hz, 2H), 7.72 (d, J = 8.1 Hz, 2H), 7.65 – 7.57 (dt, J = 8.1, 5.6 Hz, 2H), 7.44 (m, 4H), 7.37 – 7.28 (m, 4H), 6.01 (s, 2H), 2.57 (s, 6H), 1.46 (s, 6H).^{13}C NMR (100 MHz, $CDCl_3$) δ 154.53, 142.91, 141.02, 138.31, 134.02, 131.45, 130.57, 129.83, 129.45, 127.83, 126.82, 126.17, 123.62, 121.40, 120.87, 120.37, 109.64, 90.90, 85.52, 47.53, 29.16, 14.14, 8.68. MALDI-MS Calcd.m/z ($C_{39}H_{30}BF_2N_3$) 589.48, Found 589.32 (90%).

Methods and Instrumentation

^{1}H-NMR spectra were recorded on a 400MHz AVANCE spectrometer. Cyclic and differential pulse voltammetric measurements were performed on a PC-controlled electrochemical analyser (CH instruments model CHI620C). All these experiments were performed with 1 mM concentration of compounds in dichloromethane at a scan rate of 100 mV s^{-1} in which tetrabutylammoniumperchlorate (TBAP) is used as a supporting electrolyte.

Absorption and fluorescence measurements. The optical absorption spectra were recorded on a Shimadzu (Model UV-3600) spectrophotometer. Concentrations of solutions are *ca*. to be 1 x 10^{-6} M. Steady-state fluorescence spectra were recorded on a Fluorolog-3 spectrofluorometer (Spex model, JobinYvon) for solutions with optical density at the wavelength of excitation (λ_{ex}) ≈ 0.1. Fluorescence quantum yields (φ) were estimated by integrating the fluorescence bands and by using 9-phenyl-9H-carbazole (**C0**) (φ = 0.24 in CH_2Cl_2)[43] when excited at 290 nm and *N, N´*-difluoroboryl-1,3,7,9-tetramethyl-5-phenyldipyrrin (**B0**) (φ = 0.57 in CH_2Cl_2)[44] when excited at 485 nm. Fluorescence lifetime measurements were carried on a picosecond time-correlated single photon counting (TCSPC) setup (FluoroLog3-Triple Illuminator, IBH Horiba JobinYvon) employing a picosecond light emitting diode laser (NanoLED, λ_{ex} = 301 nm) as excitation source. The decay curves were recorded by monitoring the fluorescence emission maxima of the dyads (λ_{em} ≈ 345nm and 510 nm). Photomultiplier tube (R928P, Hamamatsu) was employed as the detector. The lamp profile was recorded by placing a scatter (dilute solution of Ludox in water) in place of the sample. The width of the instrument response function (IRF) was limited by the full width at half maxima (FWHM) of the excitation source, ~625 ps at 301 nm and 485 nm. Decay curves were analysed by nonlinear least-squares iteration procedure using IBH DAS6 (version 2.3) decay analysis software. The quality of the fits was judged by the χ^2 values and distribution of the residuals.MALDI-MS spectra were recorded on a TO-4X KOMPACT SEQ, KARTOS, UK, mass spectrometer. Major fragmentations are given as percentages relative to the base peak intensity.

Theoretical properties. Full geometry optimization of the **CB1**, **CB2** and **CB3**dyads wascarried out by *Gaussian 09* quantum chemical software[45] on a high speed personal computers. Density Functional Theory (DFT) was used to determine the ground state properties, while time-dependent DFT (TD-DFT) was employed for estimation of ground state to excited state transitions. B3LYP method[46] and 6-31G (d,p) basis set[47] were used to optimize the geometries of the dyads to be genuine global minimum energy structures. The geometries were used to obtain the frontier molecular orbitals (FMOs) and were also subjected to single-point TD-DFT studies (First 10 vertical singlet-singlet transitions) to obtain the UV-Vis spectra of the dyads. The integral equation formalism polarizable continuum model (PCM) within the self-consistent reaction field (SCRF) theory was used in the TD-DFT calculations to describe the solvation of the dyes in dichloromethane. The software

GaussSum 2.2.5 was employed to simulate the major portions of the absorption spectra and to interpret the nature of transitions.[48] The contribution percentages of individual units present in the dyads to the respective molecular orbitals were calculated.

Femtosecond pump-probe transient spectroscopy

Femtosecond transient absorption spectroscopy experiments were performed using an Ultrafast Femtosecond Laser Source (Libra) by Coherent incorporating diode-pumped, mode locked Ti:Sapphire laser (Vitesse) and diode-pumped intra cavity doubled Nd:YLF laser (Evolution) to generate a compressed laser output of 1.10 W. For optical detection, a Helios transient absorption spectrometer coupled with femtosecond harmonics generator both provided by Ultrafast Systems LLC was used. The source for the pump and probe pulses were derived from the fundamental output of the Libra (Compressed output 1.15 W, pulse width 100 fs) at a repetition rate of 1 kHz. The source for the pump and probe pulses were derived from the fundamental output of Libra (Compressed output 1.45 W, pulse width 100 fs) at a repetition rate of 1 kHz. About 95% of the fundamental output of the laser was introduced into a TOPAS-Prime-OPA system with 290-2600 nm tuning range from Altos Photonics Inc., (Bozeman, MT), while the rest of the output was used for generation of white light continuum. Kinetic traces at appropriate wavelengths were assembled from the time-resolved spectral data. Data analysis was performed using Surface Xplorer software supplied by Ultrafast Systems. All measurements were conducted in degassed solutions at 298 K.

Results and Discussion

Synthesis

The synthetic pathway to the target dyads,**CB1**, **CB2**, and **CB3**are exemplifiedin Scheme 1.The starting materials, **1**and **2**were synthesized as per the methods reported in the literature.[39,42] The dyad **CB1**wasaccomplished by a one-pot reaction involving the condensation of **1** with 2,4-dimethylpyrrole in presence of trifluoroacetic acid to make dipyrromethene substituted at the *meso*-position with the respective carbazole entity. Subsequent treatment of this dipyrromethene with 2,3-dichloro-5,6-dicyano-1,4-benzoquinone (DDQ), triethylamine, BF_3-etherate afforded the crude compounds as a black reaction mixture. Evaporation of the solvent and purification of this crude productover silica gel column chromatography afforded the target molecule as orange crystals.The control compound, BODIPY(**B0**), bearing no carbazole moiety, was also synthesized in the similar way. Dyads**CB2** and **CB3**were prepared via a Suzuki or Sonogashira reaction of **2** with either compound **3** or compound **4** using Pd $(PPh_3)_4$/aq Na_2CO_3 or CuI/Pd$(PPh_3)_2Cl_2$ catalyst. All precursors were quite soluble in common organic solvents, which allowed easy purification using standard chromatographic techniques. All of the newly synthesized compounds were fully characterized by ^{1}H NMR, ^{13}CNMR, ESI-MS, UV-Vis., and fluorescence spectroscopies as well as electrochemical methods. The mass spectrum of **CB1** showed a peak at *m/z* = 489 ($C_{31}H_{26}BF_2N_3$), **CB2** at *m/z* = 565 ($C_{37}H_{30}BF_2N_3$), while **CB3** at *m/z* = 589 ($C_{39}H_{30}BF_2N_3$) was ascribable to their corresponding molecular ion peaks. ^{1}H NMR spectra of **C0**, **B0**, and dyads were shown in Fig. S1-S6 and the ESI mass spectra of dyadswere shown in Fig. S7-S9.

Optical Absorption Studies

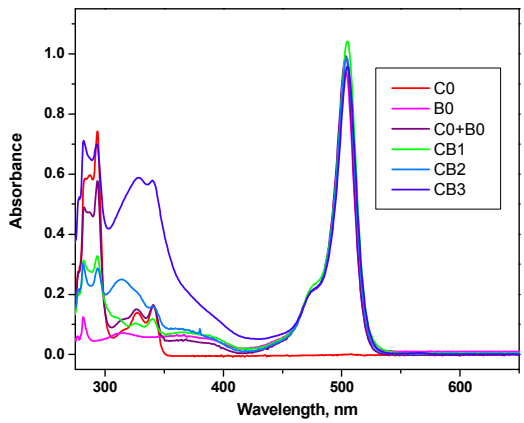

Fig. 1. Absorption spectra of the indicated compounds in toluene.

The optical absorption spectra of **CB1**, **CB2** and **CB3** dyads along with pristine**C0** and **B0**were measured in toluene as illustrated in Fig. 1. The corresponding absorption maxima (λ_{max}), and molar extinction coefficients (log ε) of the dyads (**CB1**, **CB2** and **CB3**) along with the control compounds are summarized in Table 1. The absorption maxima of the control compound, **C0** showed three peaks at 292nm, 328nm and 341 nm which was attributed to the localized aromatic π-π* transitions of the carbazole chromophores. On the other hand, reference compound, BODIPY exhibited three minor intense absorption bands between 305-400 nm, and a major intense absorption band at 501 nm corresponding to the electronic transition from the ground state to the first excited state (S_0-S_1 transition). Tethering the carbazole moiety to BODIPY chromophores did not reveal any drastic spectral changes except minor spectral changes in the UV region. Compared to pristine **C0**, the carbazole moiety in the dyads **CB1**, **CB2**, and **CB3** revealed the spectra with a split band in the UV region at 260-350 nm.[49] This spectral change may be attributed to the loss of symmetry in the carbazole framework due to the introduction of BODIPY moiety.Whereas in case of **CB1**, **CB2** and **CB3** dyads, the absorption peaks between 290 – 450 nm were blue shifted (~10 – 20 nm) compared to the control compounds, **B0** and **C0**, displaying minor ground state interactions within the chromophores in all the dyads. Moreover, the characteristic peak of **CB1**at 502nm, and**CB2** and C**B3** at 503 nm corresponding to the BODIPY moiety was red shiftedby ~ 1-2 nm compared to the pristine**B0** having

absorption maxima at 501 nm. More essentially, the stronger absorption of BODIPYbetween 420–530 nm (λ_{max} =501 nm) had no overlap with the carbazole absorption in this wavelength range indicating that irradiation of the dyads at 485 nm would selectively excite the BODIPY moiety of the dyads.

Table 1 Absorption and electrochemical data.

compound	Absorption, λmax, nm (log ε, M^{-1} cm^{-1})[a]	Potential V vs SCE[b] oxidation	reduction
C0	292 328 341 (3.13) (0.77) (0.85)	1.30	-
B0	318 363 501 (0.46) (0.40) (6.76)	1.22	-0.97
CB1	293 324 339 502 (4.23) (1.39) (1.55) (13.05)	1.21, 1.54	-1.20
CB2	293 310 349 503 (3.18) (2.56) (1.59) (9.63)	1.20, 1.50	-1.21
CB3	293 328 341 503 (12.55)(10.89) (10.28) (15.07)	1.28, 1.53	-1.15

[a]Solvent= Toluene. Error limits: λ_{max}, ±1 nm; log ε, ±10%. [b]CH_2Cl_2, 0.1 M TBAP. Glassy carbon working electrode; standard calomel electrode is reference electrode, Pt electrode is auxiliary electrode. Error limits, $E_{1/2}$ ± 0.03 V.

Electrochemical Studies.

The electrochemical behaviour of **CB1**, **CB2** and **CB3** dyads was explored withcyclic and differential pulse voltammetric techniques. Fig. 2 demonstrates the differential pulse voltammograms of **CB1**, **CB2**, and **CB3** dyads along with the control compounds (**C0** and **B0**) measured in dichloromethane containing 0.1 M TBAP as supporting electrolyte. The corresponding redox potential data are summarized in Table 1.

The investigated dyads showed two oxidation and one reduction processes under the experimental conditions employed. **B0** exhibited a reversible one-electron oxidation at $E_{1/2}$ = 1.21 V vs SCE and a reversible one electron reduction $E_{1/2}$ = -0.97 V. The other control compound **C0** exhibited one electron oxidation at 1.30 V and no reduction was observed within the potential window of the solvent. In all three dyads, a reversible oxidation at ~1.25 V vs SCEwas observed belonging to the oxidation of BODIPY and a second oxidation process at higher potential due to carbazole oxidation. On the other hand, one reversible reduction was observed in case of **CB1** and **CB2** dyads at -1.20 V and the origin of this peak was due to the reduction of the BODIPY moiety of the dyad. The reduction potential of the dyads was anodically shifted by 200 mV when compared to pristine **B0** revealing the influence of carbazole in modulating the redox potentials.

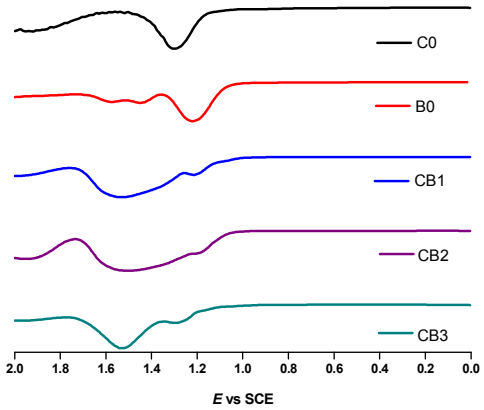

Fig. 2. Differential pulse voltammograms of oxidation of the indicated compounds in CH_2Cl_2 containing 0.1 M (n-$C_4H_9)_4NClO_4$. The concentrations of the dyads were held at 1 mM; scan rate = 100 mVs^{-1}.

Computational Studies.

To gain insight into the electronic properties of the dyads with π-conjugated spacers, we carried out DFT and TD-DFT calculations for **CB1**, **CB2** and **CB3**D-Asystems with functional basis set of B3LYP/6-31G (d,p) level. The orbital energy levels in vacuum, minimum energy conformation and electron density plots are shown in Table 2. For all the examined dyads, it was observed that the carbazole moiety, in its neutral state wasplanarand was perpendicular to the BODIPY plane as shown in the optimized structures in Table 2. As a result, carbazole lost its symmetry as it reflected in absorption properties (See section 3.2). The edge-to-edge and centre-to-centre distances ($R_{c\text{-}c}$) between the CBZ and BODIPY moieties in the dyads were estimated and summarized in Table 3. In the molecular electrostatic potential (MEP) maps, for all the dyads, the positive electrostatic potential was at the CBZ and spacer connecting the chromophores, while the negative potential was concentrated at the pyrrolic –NH and $–BF_2$ groups of BODIPY. Frontier highest occupied molecular orbitals (HOMO and HOMO-1) and lowest unoccupied molecular orbitals (LUMO and LUMO+1) for the **CB1**, **CB2** and **CB3** dyads are shown in Table 2. In these dyads, the HOMO was located on the BODIPY π-system, importantly; parts of the HOMO andLUMO were also located on the phenyl spacer, suggesting a notable interaction between donor and spacer entities.However, it should be noted from the electronic distribution of

Table 2 Optimized Structures, Electrostatic Potential Maps,and Plots of Frontier Molecular Orbitals.

	CB1	CB2	CB3
Optimized structure	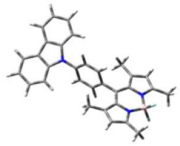	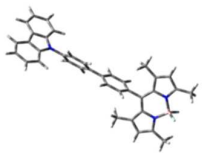	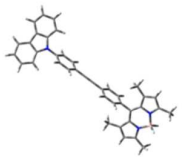
Electrostatic potential map (ESP)	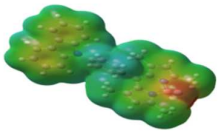		
LUMO+1	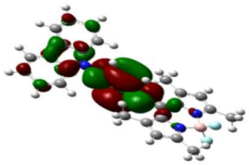	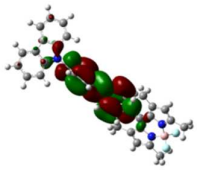	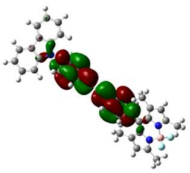
LUMO	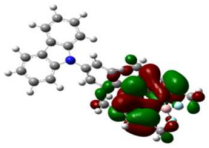	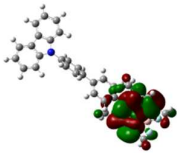	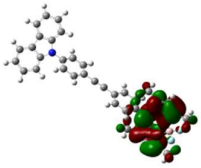
HOMO	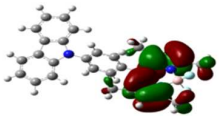	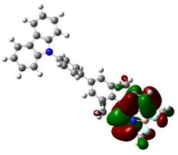	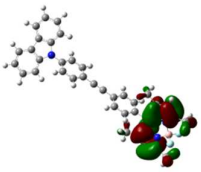
HOMO-1	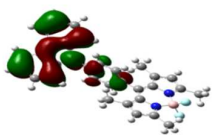	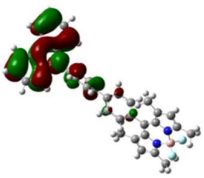	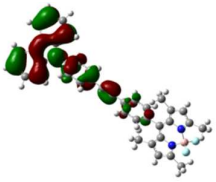

frontier orbitals that the interaction between donor and acceptor is weaker in case of all the three dyads. The calculated gas phase HOMO–LUMO gap was found to be 2.99, 3.00 and 2.97 eV for **CB1**, **CB2**, and **CB3**, respectively.

Based on the experimental observations, TD-DFT studies of these molecules were carried out using B3LYP energy functional with the 6-31G (d,p) basis set in order to gain a deeper understanding of the excited-state transitions within the framework of the polarizable continuum model (PCM) in dichloromethane solvent. These results are in reasonable agreement with the experimental values. The singlet state properties of maximum wavelength absorbance, oscillationstrength (*f*), excited state energy (*E*) in eV and the

Table 3 B3LYP/6-31G (d,p)-Optimized Distances between CBZ and BODIPY Moieties and Related Orbital Energies in the Investigated Dyads.

Dyads	*E*, K·cal/mol	$R_{e\square e}$, Å	$R_{c\square c}$, Å	HOMO−1, eV	HOMO (H), eV	LUMO (L), eV	LUMO+1, eV	H−L gap, eV
CB1	-9.95 x 10^5	5.72	10.33	-5.55	-5.43	-2.44	-0.89	2.99
CB2	-11.40 x 10^5	10.05	14.66	-5.45	-5.40	-2.40	-1.33	3.00
CB3	-11.87 x 10^5	12.61	17.22	-5.43	-5.39	-2.42	-1.75	2.97

percentage contribution of molecular orbital of all three dyads by means of absorption spectraare presented in Supporting Information. Theoretical absorption spectra of **CB1** and **CB2**, in **CB3**, see insupporting information (Fig. S10) of each dyad segment was computed from the frontier molecular orbitals using the *GaussSum* software.

Excited State Properties

Unlike the ground state properties, the excited state properties of dyads were different from its control compounds. First, the photochemical behaviour of the Carbazole-BODIPY dyads was investigated, using steady-state fluorescence measurements. When equimolar solutions of the dyads and the control compounds were excited at 290 nm in toluene, i.e., the λ_{max} corresponding to predominant absorption of CBZ, the emission peak (λ_{max}: ~350 nm) corresponding to the CBZ moiety was found to be fully quenchedin case of the dyadswhen compared to their individual constituent, **C0** (see Fig. 3). A similar fluorescence quenching was also observed in other investigated solvents with increasing polarity. The corresponding emission maxima and quantum yields are presented in Table 4. The $E_{0\text{-}0}$ (0-0 spectroscopic transition energy) values of the CBZ (3.54±0.05 eV) and BODIPY (2.41±0.05eV) moieties of the dyads, as estimated from an overlap of their absorption and emission spectra, were found to be in the same range as the $E_{0\text{-}0}$ values of **C0** and **B0**, respectively.Inaddition to the quenching of CBZ peak, when excited at 290 nm, appearance of a new emission band corresponding to the BODIPY moiety around 515 nm was also observed. Under these conditions, when an equimolar solution of only **B0** was excited at 290 nm, very weak emission of BODIPY at 515 nm was observed. These control experiments and quenching of the emission intensity of the CBZ moiety and appearance of BODIPY emission bands in these dyads clearly indicate occurrence of photoinduced energy transfer (PEnT). Figure 3 also suggests that the emission intensity of BODIPY moiety of dyads, observed because ofPEnT from ^{1}CBZ* to BODIPY, follows the order:**CB1**>**CB2**>**CB3**, as the distance between donor and acceptor increased. Similar quenching behaviour was also observed when the dyads were excited at 340 nm exciting predominantly CBZ.

Further, using time-correlated single photon counting technique, excited state lifetime of dyads and its individual constituent **C0**was performed. Figure 4 exemplified excited

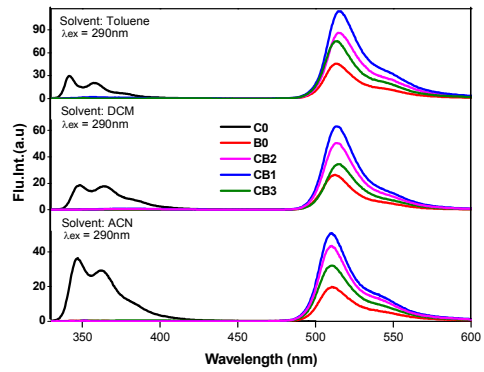

Fig. 3. Fluorescence spectra (λ_{ex} = 290 nm)of equimolar solutions of **C0**, **CB1**, **CB2**, and **CB3** in toluene, DCNM, and acetonitrile solvents.

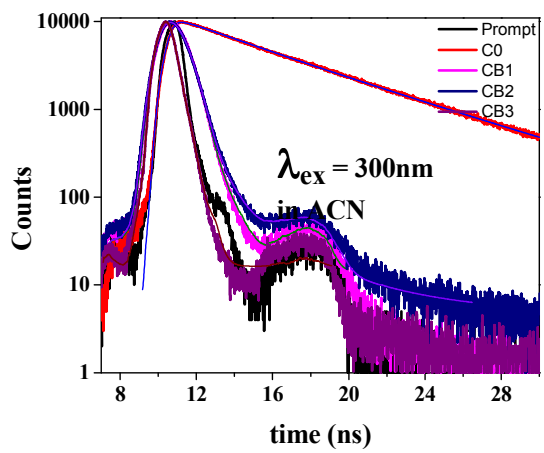

Fig. 4. Fluorescence decay curves of **C0**, **CB1**, **CB2**, and **CB3** (λ_{ex}= 300 nm) in acetonitrile solvent.

state emission decay profile of the dyads collected in acetonitrile, by selectively exciting samples at λ_{ex} = 300 nm, where the CBZ absorb predominantly. As expected, when CBZ emission at λ_{em} = 350 nm was monitored, the fluorescence lifetime (τ) of three dyads were quenched in all investigated solvents, when compared to **C0** (Table 4). More interestingly,

Table 4 Fluorescence and life-time data.[a]

Compound	λ_{em}, nm (Φ , %Q)[d]			λ_{em}, nm[b] (Φ)[d]			λ_{ex} = 300 nm,τ,[e] ns, (A%)		
	Toluene	DCM	ACN	Toluene	DCM	ACN	Toluene	DCM	ACN
C0[b]	341, 358 (0.210)	348, 364 (0.243)	346, 362 (0.252)	-	-	-	6.22	6.45	6.43
B0[c]	-	-	-	512 (0.540)	512 (0.570)	509 (0.612)	-	-	-
CB1[b]	- (0.008, 96)	- (0.006, 97)	- (0.002, 98)	515 (0.712)	514 (0.723)	512 (0.789)	0.20	0.24	0.21
CB2[b]	357, 373 (0.022, 89)	- (0.006, 97)	- (0.002, 98)	515 (0.685)	514 (0.689)	511 (0.688)	0.42 (89) 1.69 (11)	0.16	0.12 (98) 0.46 (02)
CB3[b]	- (0.012, 88)	- (0.015, 93)	- (0.003, 96)	514 (0.644)	515 (0.652)	511 (0.648)	0.11 (97) 1.06 (03)	0.25	0.28

[a]Spectra were measured at 293±3 K. [b]λ_{ex} = 290 nm. [c]λ_{ex} = 485 nm. [d]Error limits: λ_{em}, ± 1 nm; Φ_f, ± 10%.[e]All lifetimes are in nanoseconds.

as the data from Table 4 shows,increasing the polarity of the solvent increased the quenching efficiency. Fluorescence quenching efficiency Q, can be approximately estimated as follows:

$$Q = \frac{\phi(Ref) - \phi(Dyad)}{\phi(Ref)} \quad (1)$$

$$k_{obs} = \frac{Q/(1-Q)}{\tau(C0)} \quad (2)$$

Where $\Phi_{(Ref)}$ and $\Phi_{(Dyad)}$ refer to the fluorescence quantum yields for **C0** and the dyads. $\tau_{(C0)}$is the singlet-state lifetime of C0 (6.22, 6.45, 6.43 ns, in toluene, DCM, and CH_3CN, respectively, see Figure S12). The rate of fluorescence quenching, k_{obs}, estimated using the fluorescence data are presented in Table 5.

Further evidence for PEnT was secured from recording excitation spectra of the dyads. The excitation spectra were recorded by monitoring the emission at 515 nm corresponding to BODIPY moiety and scanning the excitation wavelength. Therecorded spectra revealed CBZ peaks in UV region, similar to the absorption spectra of the dyads (Fig. 5). Energy transfer efficiencies, $k_{EN}(obs)$, that are obtained by comparing an overlap of excitation and absorption spectra in each investigated solvent are collected in Table 3 and spectra showing this overlap for both the dyads are illustrated in Figure 4. Table 3 also contains data on $k_{EN(obs)}$ values where

$$k_{EN}(obs) = \frac{T_{obs}/(1-T_{obs})}{\tau(CBZ)} \quad (3)$$

Theoretical considerations

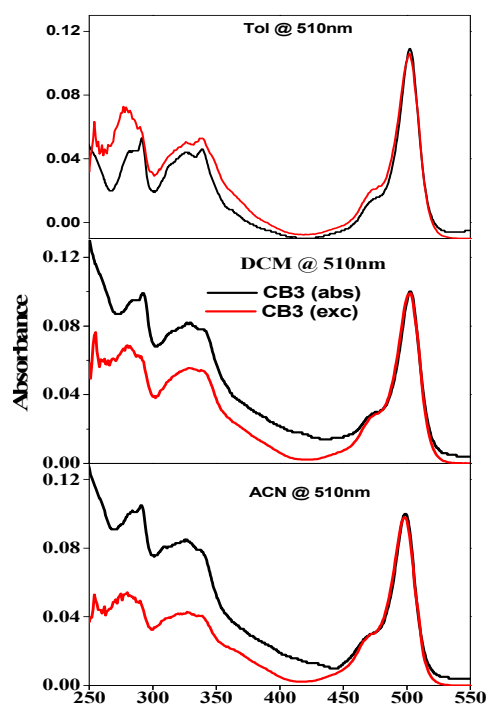

Fig. 5. Overlay of the absorption (——) and excitation (———) spectra of the dyads. The excitation spectra were corrected for the instrument response function and were normalized with respect to the absorption spectra as described in Ref. [56].

Table 5. Energy transfer data[a]

Compound	Solvent	%Q	%T	k_{obs} ($10^9 s^{-1}$)	$k_{EN(obs)}$ ($10^{10} s^{-1}$)[c]	J^d (cm^6 $mmol^{-1}$)[d]	$k_{Förster}$ (10^{10} s^{-1})[e]
CB1	Toluene	96	82	3.85	0.73	1.03×10^{-14}	33.11
CB2	(η = 1.49, ε = 2.38)[b]	89	80	1.30	0.64	0.99×10^{-14}	3.89
CB 3		95	86	3.05	0.98	0.91×10^{-14}	1.36
CB1	CH_2Cl_2	97	93	5.01	2.06	1.29×10^{-14}	56.43
CB2	(η = 1.45,ε = 8.93)[b]	93	90	2.06	1.39	1.23×10^{-14}	6.58
CB3		96	82	3.72	0.70	1.16×10^{-14}	2.36
CB1	CH_3CN	98	97	7.62	5.03	1.22×10^{-14}	70.02
CB2	(η = 1.34,ε = 37.50)[b]	95	95	2.95	2.94	1.19×10^{-14}	8.36
CB3		99	89	15.39	1.26	1.08×10^{-14}	2.89

[a]Error limits: %Q, k_{obs}±8%, %T, $k_{EN}^{(obs)}$: ±15% [b]n and ε refer to refractive index and dielectric constant of the solvents, respectively. [c]κ^2 = 0.66 in all the cases and $R_{c\text{-}c}$ = 10.33 Å **(CB1)**, 14.66 Å **(CB1)**, and 17.22**(Dyad 2)**. [d]Spectral overlap term calculated by using PhotochemCAD software.[52] [e]$k_{EN}^{(obs)}$ calculated by using equation $\frac{Tobs/(1-Tobs)}{\tau(CBZ)}$

T_{obs}, energy transfer

Energy transfer in bichromophoric π-conjugated systems can be triggered by mainly two types of mechanisms, Förster mechanism (or dipole-dipole interaction)[50] or the Dexter mechanism (or electron exchange mechanism).[51] In Förster mechanism, the rate of energy transfer to be proportional to spectral overlap, *J*, of the donor emission and acceptor absorption, and can be calculated using following equation.

$$J_{Forster} = \frac{\int F(\nu)\varepsilon(\nu)\varepsilon^{-4}d\nu}{\int F(\nu)d\nu} \quad (4)$$

F(ν) is the normalized fluorescence intensity of the energy donor at wave number ν (cm^{-1}), and ε ($mmlo^{-1}$ cm^{-1}) is the molar extinction coefficient of energy acceptor. In the present study, $J_{Förster}$for **CB1**, **CB2**, and **CB3** in three different solvents were calculated using software, *PhotochemCAD*[52] and obtained values are tabulated in Table 5. In these D-A systems, the calculated $J_{Förster}$ were found to be in the range of $1.03 \times 10^{-14} – 1.30 \times 10^{-14}$ cm^6 $mmol^{-1}$ (or M^{-1} cm^3) depending on the polarity of the solvent. The Förster mechanism predicts the rate constant, $k_{Förster}$, by means of the following equation (5)

$$k_{Foster} = \frac{8.8x10^{23}\kappa^2\phi_D J_{Foster}}{n^4\tau_D R^6} \quad (5)$$

Hereη is the solvent refractive index, Φ_D and τ_D are the emission quantum yield and lifetime of the isolated donor in various solvents (see Table 5 and Fig. S12), R_{DA} is the donor-acceptor centre-to-centre distance (from Table 3, 10.33 Å for **CB1**, 14.66 Å for **CB2** and 17.22 Å for **CB3**), and κ^2, the orientation factor, taking into accountthe relative orientation of the transition dipole moments of the donor and the acceptor and for randomly oriented dipoles a value of κ^2 = 2/3 is generally used. The rate of Förster energy transfer, $k_{Förster}$, increases as the polarity of the solvent increases in all three dyads. From Table 5, it can be observed that in **CB2** and **CB3**, $k_{EN}^{(obs)}$ values both in non-polar and polar solvents are comparable with calculated results, supporting Förster type mechanism. On the other hand, in **CB1** dyad, $k_{EN}^{(obs)}$ values both in non-polar and polar solvents are not comparable with calculated results.This could be due to close proximity between the donor and acceptor or the approximations involved in theoretical estimates.

The free-energy changes (ΔG_{EN}) accompanying energy transfer by dipole-dipole mechanism in all solvents, was calculated by eq 6[53] and tabulated in Table 6.

$$\Delta G_{EN} = -E_{00}(CBZ^*) + E_{00}(BODIPY^*) \quad (6)$$

Table 6: Free-energy changes (in eV) for singlet energy transfer (ΔG_{EN}) for the investigated dyads in solvents of varying polarity.

Compound	ΔG_{EN}(^{1}CBZ*-BODIPY)		
	Toluene	DCM	ACN
CB1	-1.10	-1.13	-1.13
CB2	-1.11	-1.09	-1.09
CB3	-1.06	-1.02	-1.05

Next, femtosecond transient absorption spectral studies were performed in toluene to secure evidence of excited state energy transfer. The samples were excited at 340 nm where majority of

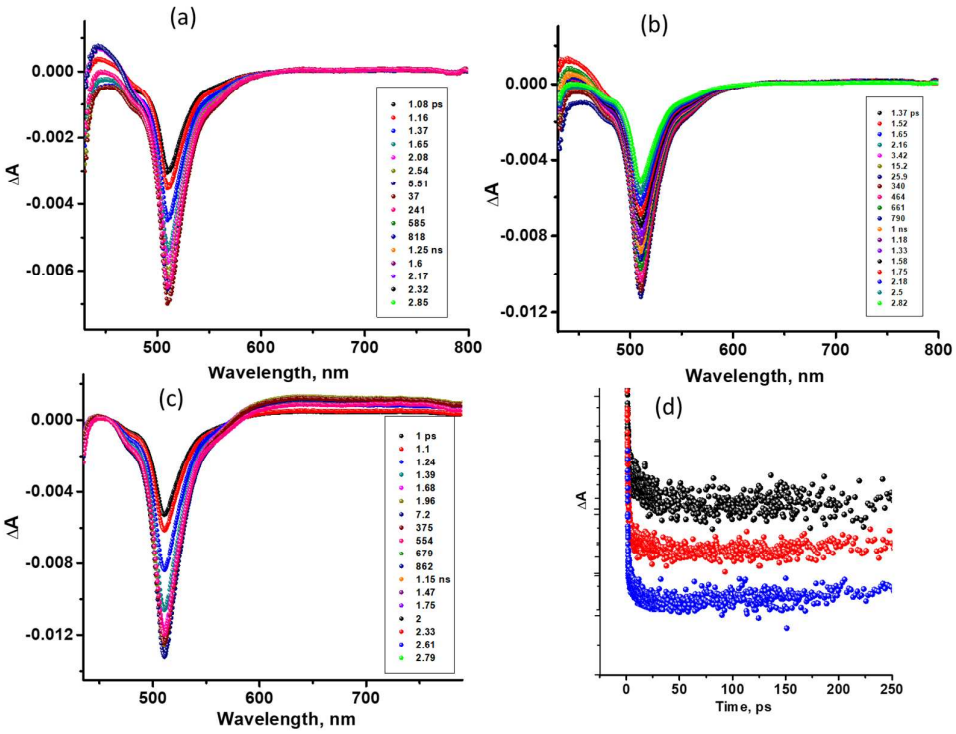

Fig. 6: Femtosecond transient absorption spectra at the indicated delay times of (a) **CB1**, (b) **CB2** and (c) **CB3** in toluene at the excitation wavelength of 340 nm. Figure (d) shows growth profile of the 520 nm peak of BODIPY used to estimate the energy transfer rate constants (—) **CB1**, (—) **CB2**, and (—) **CB3**.

the absorbance was from the carbazole entity. First, in a control experiment pristine BODIPY, **B0** was excited at 502 nm in toluene whose spectra at different delay times are shown in Fig. S13 in SI. The main feature involved a negative transient peak at 510 nm having contributions from ground state bleaching and stimulated emission.[54,55] The recovery of this peak was slow that was in agreement with relatively longer fluorescence lifetime of BODIPY, being 2.67 ns (*vide supra*). In contrast, excitation of control BODIPY, **B0** at 340 nm where BODIPY absorbance was minimal revealed very weak ill-defined transient peaks in the region where BODIPY transient peaks are expected (see Fig. S14 in SI). Control carbazole, **C0** was also excited at this wavelength and the transient spectra at different delay times are shown in Fig. S15. The transient spectra had broad features covering the 500-720 nm region with peak maxima at 635 nm due to transitions originating from ^{1}CBZ*. In accordance with long lifetime of ^{1}CBZ* (6.22 ns in toluene, *vice supra*), the decay of the transient peak was rather slow.

The transient absorption spectra of the investigated dyads at the excitation wavelength of 340 nm in toluene are shown in Figure 6a-c. The spectral features were similar to what was observed for **B0** when it was directly excited at 502 nm. The evolution of strong BODIPY transient peaks (in contrast to weak ill-defined peaks observed for pristine **B0** at this excitation wavelength) is indicative of efficient singlet-singlet energy transfer. That is, rapid transition from ^{1}CBZ*-BODIPY to form CBZ-^{1}BODIPY* was witnessed. For **CB1** and **CB2**, no peak of ^{1}CBZ* at 635 nm was observed indicating very efficient energy transfer, however, for **CB3**, weak positive peak at 635 nm was observed whose decay was accompanied by growth of BODIPY peak at 520 nm. By estimating the time constants forgrowth of the 520 nm peak (see Figure 6d), the rate constants for energy transfer were estimated. The rate of energy transfer, k_{ENT} thus estimated was found to be 2.0 x 10^{10} s^{-1} for **CB1**, 1.3 x 10^{10} s^{-1} for **CB2**, and 0.8 x 10^{10} s^{-1} for **CB3** (experimental error = + 10%). Thedifference from experimental k_{ENT} from that theoretically estimated one in Table 5 could be attributed to the employed approximations, especially for κ^2 value, and the experimental error with the k_{ENT} measurements.

Excitation of the dyads at 485 nm corresponding to BODIPY revealed marginal decrease in emission intensities. Additionally, free-energy calculations performed for photoinduced electron transfer from ^{1}BODIPY* to CBZ were found to be endothermic in all three cases. Hence, no further studies were performed.

Conclusions

Insummary, we have designed, synthesized and characterized a series of Carbazole-BODIPY dyads in which donor carbazole tethered with acceptor BODIPY using spacers of varied sizes *i.e.*, phenyl bridge, biphenyl bridge and diphenylethyne bridge. Optical

and electrochemical properties suggested that there were minimal ground state interactions between the chromophores in these dyads. Photophysical studies of these dyads showed that selective excitation of the carbazole moiety results in very efficient energy transfer process. The rate constants for energy transfer, k_{ENT}, measured from femtosecond transient absorption technique in toluene was found to be in the range of 0.8 – 2.0 x 10^{10} s^{-1}, depending on the type of spacer between the CBZ and BODIPY entities. These experimental k_{ENT} values were in close agreement with the theoretically estimated ones. On the other hand, no photochemical events were observed from ^{1}BODIPY* in these dyads.

Acknowledgements

We are grateful to the Department of Science and Technology (DST, SB/S1/IC-14/2014), and National Science Foundation (grant 1401188 to FD) for financial support. GR and DN thank, RMIT and CSIR, respectively, for research fellowships.

References

1. M. Llansola-Portoles, D. Gust, T. A. Moore, A. L. Moore, *C. R. Chimie* 2017, **3**, 296-313.
2. J. Su, L. Vayssieres, *ACS Energy Lett*. 2016, **1**, 125-131.
3. G. Knör, *Coord. Chem. Rev*., 2015, **304-305**, 102-108.
4. J. Barber, P. D. Tran, *J. R. Soc. Interface* 2013, 10: 20120984.
5. O. Ito, F. D'Souza,*Molecules* 2012, **17**, 5816-5835.
6. I. McConnell, G. Li, G. W. Brudvig, *Chem. Biol*. 2010, **17**, 434–447.
7. J. Kandhadi, V. Yeduru, P. R. Bangal, L. Giribabu, *Phys.Chem.Chem.Phys*. 2015, **17**, 26607-620.
8. K. Sudhakar, S. Gokulnath, L. Giribabu, G. N. Lim. T. Tram, F. D'Souza,*Chem. Asian J.* 2015, **10**, 2708-2719.
9. N. Karakostas, A. Kaloudi-Chantzea, E. Martinou, K. Seintis, F. Pitterl, H. Oberacher, M. Fakis, J. K. Kallitsisd, G. Pistolis, *Faraday Discuss*., 2015, **185**, 433-454.
10. T. Lazarides, S. Kuhri, G. Charalambidis, M. K. Panda, D. M. Guldi, A. G. Coutsolelos, *Inorg. Chem*. 2012, **51**, 4193-4204.
11. L. Giribabu, T. A. Rao, B. G. Maiya. *Inorg. Chem*. 1999, **38**, 4971-4980.
12. D. Kuciauskas, P. A. Liddell, S. Lin, T. E. Johnson, S. J. Weghorn, J. S. Lindsey, A. L. Moore, T. A. Moore, D. Gust. *J. Am. Chem. Soc*., 1999, **121**, 8604-8614.
13. M. R. Singh, A. T. Bell, *Energy Environ. Sci.,*2016, **9,** 193–199.
14. C. B. KC, F. D'Souza,*Coord. Chem. Rev*. 2016, **322**, 104-141.
15. N. V. Krishna, J. V. V. Krishna, S. Singh, L. Giribabu, L. Han, I. Bedja, R. K. Gupta, A. Islam, *J. Phys.Chem. C* 2017, 121, 6464-6477.
16. M. R. Topka, P. H. Dinolfo, *ACS Appl. Mater. Interfaces* 2015, **7**, 8053–8060.
17. N. Duvva, K. Sudhakar, D. Badgurjar, R. Chitta, L. Giribabu, *J. Photochem. Photobiol., A* 2015, 312, 8–12.
18. M. J. Leonardi, M. R. Topka, P. H. Dinolfo, *Inorg. Chem*. 2012, **51**, 13114– 13122.
19. B. C. Popere, A. M. D. Pelle, S. Thayumanavan, *Macromolecules* 2011, **44**, 4767–4776.
20. K. Jain, N. Duvva, D. Badgujar, L. Giribabu, R. Chitta, *Inorg. Chem. Commun*. 2016, **66**, 5–10.
21. Z.-B. Sun, M. Guo, C.-H. Zhao, *J. Org. Chem*. 2016, **81**, 229–237.
22. S. Kumar, H. B. Gobeze, T. Chatterjee, F. D'Souza, R. Ravikanth, *J. Phys. Chem. A* 2015, **119**, 8338-8348.
23. S. P. Singh, T. Gayatri, *Eur. J. Org. Chem*. 2014, **7**, 4689–4707.
24. D. Gust, T. A. Moore, K. M. Kadish, K. M. Smith, R. Guilard (Eds.), *The PorphyrinHandbook*, vol. 8, Academic Press, San Diego, 2000, pp. 153–190.
25. F. Diederich, M. Go´ımez-Lo´pez, *Chem. Soc. Rev.* 1999, **28**, 263–277.
26. L. Giribabu, Ch. Vijay, P.Y. Reddy, *Chem. Asian J*. 2007, 2, 1574–1580.
27. A.J. Jimenez, F. Spanig, M. S. Rodrıguez-Morgade, K. Ohkubo, S. Fukuzumi, D. M. Guldi, T. Torres, *Org. Lett.* 2007, 9, 2481–2484.
28. T. H. Ngo, D. Zieba, W. A. Webre, G. N. Lim, P. A. Karr, S. Kord, S. Jin, K. Ariga, M. Gali, S. Goldup, H. P. Hill, F. D'Souza,*Chem. Eur. J*. 2016, **22**, 1301-1312.
29. L. Giribabu, K. Jain, K. Sudhakar, N. Duvva, R. Chitta, *J. Luminescence* 2016, **177**, 209-218.
30. F. D'Souza, P. M. Smith, L. Rogers, M. E. Zandler, D.-M. ShafiqulIslam, Y. Araki, O. Ito, *Inorg. Chem*. 2006, **45**, 5057–5065.
31. J. L. Sessler, D. Seidel, *Angew Chem. Int. Ed.* 2003, **42**, 5134-5175.
32. Y. Rio, W. Seitz, A. Gouloumis, P. Vasquez, J. L. Sessler, D. M. Guldi, T. Torres. *Chem. Eur. J.* 2010, **16**, 1929-1940.
33. M. E. El-Khouly, S. Fukuzumi, F. D'Souza,*ChemPhysChem* 2014, **15**, 30-47.
34. A. Loudet, K Burgess, *Chem. Rev*. 2007, 107, 4891-4932.
35. T. G. Terazono, Kodis, P. A. Liddell, T. A. Moore, A. L. Moore, D. Gust, *J. Phys. Chem. B* **2**009, **113**, 7147-7155.
36. F. D'Souza, P. M. Smith, M. E. Zandler, A. L. McCarty, M. Itou, Y. Araki, O. Ito, *J. Am. Chem. Soc*., 2004, **126**, 7898-7907.
37. K. Srinivas, Ch. R. Kumar, M. A. Reddy, K. Bhanuprakash, V. J. Rao, L. Giribabu, *Syn. Metals* 2011, **161**, 96-105.
38. N. Duvva, R. K. Kanaparthi, J. Kandhadi, G. Marotta, P. Salvatori, F. DeAngelis, L. Giribabu, *J. Chem. Sci*., 2015, **127**, 383-394.
39. S. H. Kim, I. Chao, M. K. Sim, S. Park, S. Y. Park, *J. Mater. Chem*. 2011, 21, 9139-9148.
40. B. L. Hu, F. Zhuge, X. J. Zhu, S. S. Pen, X. X. Chen, L. Pan, Q. Yan, R. Li. *J. Mater. Chem*. 2012, 22, 520-526.
41. M. Kollmannsberger, K. Rurack, U. Resch-Genger, J. Daub, *J. Phys. Chem. A*, 1998, **102**, 10211-10220.
42. C. Gol, M. Malkoc, S. Yesilot, M. Durmus, *Dyes & Pig*. 2014, **111**, 81-90.

43. G. E. Johnson, *J. Phys. Chem*. 1980, **84**, 2940-2946.
44. A. Loudet, K. Burgess, *Chem. Rev*., 2007, **107**, 4891-4932.
45. M. J. Frisch, G. W. Trucks, H. B. Schlegel, G. E. Scuseria, M. A. Robb, J. R. Cheeseman, G. Scalmani, V. Barone, B. Mennucci, G. A. Petersson, et al. *Gaussian 09*, revision B.01; Gaussian, Inc.: Wallingford, CT, 2010.
46. A. D. Becke, *J. Chem. Phys*. 1993, **98**, 1372−1378.
47. G. A. Petersson, M. A. Al-Laham, *J. Chem. Phys*. 1991, **94**, 6081−6091.
48. M. Cossi, V. Barone, R. Cammi, Tomasi, J. *Chem. Phys. Lett*. 1996, **255**, 327−335.
49. S. M. Bonesi, R. Erra-Balsells, *J. Lumines*. 2001, **93**, 51-74.
50. Th.Förster, 10th Spiers Memorial Lecture, *Discuss. Faraday Soc*. **1959**, *27*, 7-17.
51. D. L Dexter, *J. Chem. Phys*. 1953, **21**, 836-850.
52. H. Du, R. –C. A. Fuh, J. Li, L. A. Corkan, J. S. Lindsey, *Photochem. Photobiol*. 1998, **68**, 141-142.
53. J. J. Snellenburg, S. P. Laptenok, R. Seger, K. M. Mullen, I. H. M. vanStokkum, *J. Stat. Soft*. 2012, **49**, 1−22.
54. M. E. El-Khouly, A. N. Amin, M. E. Zandler, S. Fukuzumi, F. D'Souza,*Chem. - Eur. J*. 2012, **18**, 5239−5247.
55. C. A. Wijesinghe, M. E. El-Khouly, N. K. Subbaiyan, M. Supur, M. E. Zandler, K. Ohkubo, S. Fukuzumi, F. D'Souza,*Chem. - Eur. J*. 2011, **17**, 3147−3156.
56. L. Giribabu, B. G. Maiya, *Res. Chem. Intermed*. 1999, **25**, 769-788.

TOC

Photoinduced Energy Transfer in Carbazole-BODIPY Dyads

Govind Reddy, DuvvaNaresh, Sairaman Seetharaman, Francis D'Souza Lingamallu Giribabu